ID 1211

30TH INTERNATIONAL COSMIC RAY CONFERENCE

Snapshot Observations and Time-resolved Modeling of Gamma-ray Blazars during Major Flares

J.E. CARSON[1], J. CHIANG[1]

[1]*Stanford Linear Accelerator Center, 2575 Sand Hill Road, Menlo Park, CA 94025, USA*
carson@slac.stanford.edu, jchiang@slac.stanford.edu

Abstract: Major blazar flares likely result from injections of relativistic pair plasma into the inner jets. Quantifying the jet's basic physical parameters has been hampered by the modest sensitivity of past observations, which have allowed only time-averaged pictures of these rapidly changing phenomena. The capabilities of gamma-ray observatories have dramatically improved recently with H.E.S.S. and MAGIC, and the improvements continue in 2007 with the advent of VERITAS and the Large Area Telescope (LAT, 30 MeV $<$ E $<$ 300 GeV) aboard GLAST. These instruments can measure the spectra of flaring blazars on time scales of hours or less, shorter than the expected cooling time scales of the pair population in some cases. Using a sophisticated code based on the work of M. Böttcher and extended by us, we explore the effects of various cooling mechanisms and jet physical conditions on the SED "snapshots" that are possible with joint LAT/TeV observations. The code includes cooling via synchrotron, synchrotron self-Compton, and external Compton radiation, allows for finite jet injection times, and evolves the pair population self-consistently as it cools after a major flare.

The Model

The model of Böttcher et al. (1997) [1] and Böttcher & Bloom (2000) [2] form the basis for the analyses presented here. In this model (see Figure 1), pair plasma blobs are instantaneously injected into a cylindrical jet structure with bulk relativistic motion. The electrons have an initial power-law distribution over a range of energies (γ_{min}, γ_{max}). The broad line region (BLR) is also included with an optical depth τ. The following radiation processes are considered: synchrotron emission (Synch), inverse-Compton scattering of synchrotron photons (SSC), inverse-Compton scattering of radiation from the accretion disk entering the jet directly (ECD), and inverse-Compton scattering of accretion disk radiation scattered off broad-line region clouds (ECC). An important feature is that the electron distribution is evolved self-consistently as the particles cool, allowing for properly time-averaged spectra to be generated.
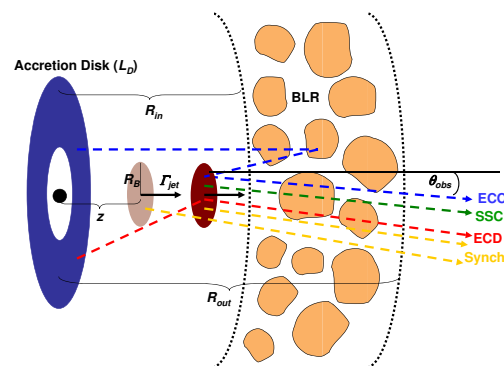
Figure 1: Cartoon of the leptonic emission model discussed in this paper, with radiation contributed from synchtron (Synch), synchrotron self-Compton (SSC), and external inverse-Compton emission (ECC, ECD).

Synchrotron/SSC Modeling

Here we use the model to explore the shape of the instantaneous and time-averaged SEDs for a BL Lac-type jet, i.e., one with no external sources of seed photons. In particular, we consider the Synch-SSC model that has been fit to a recent, very bright flare of Markarian 501 (Mrk 501) as observed by the MAGIC telescope (Albert *et al.* 2007 [3]).

In June–July 2005, two major flares from Mrk 501 were observed by MAGIC with temporal resolution of several minutes [3]. These flares exhibited variability time scales of order $\sim$ 10 minutes, shorter than had been previously seen for any blazar at gamma-ray energies. The data during the flares were fit to an instantaneous Synch-SSC model, and the model parameters were adjusted to pass through the MAGIC data and contemporaneous, but not strictly simultaneous, X-ray (RXTE/ASM) and optical (KVA telescope) data.

We have taken the model parameters from the Albert *et al.* fit for to June 30 flare as input to our time-evolution code, and we plot the SEDs we obtain in Figure 2. Our initial instantaneous SED (topmost solid curve) matches the SED found by Albert *et al.*(see their Figure 21), modulo some details having to do with the synchrotron emission kernel used. However, the time-averaged spectrum (dashed curve) has a very different shape and magnitude than the time-resolved ones. The high-energy peak tends to move towards lower energies as the model integrates over longer times, a reflection of the fact that the higher-energy electrons cool faster than the lower-energy ones; both peaks flatten considerably with time averaging; and most importantly for these data, the magnitude of the SEDs decrease as the pair population losses energy. As a consequence, the time-averaged spectrum under-predicts the higher energy peak by nearly an order of magnitude. This calculation highlights a major conclusion of this work: models that properly evolve the electron population are essential, and fits to instantaneous models can yield misleading and unreliable results. Since the MAGIC spectra comprise data integrated over the entire flare, a time-averaged SED calculation should be used for ascertaining the model parameters.

In order to compensate for the order-of-magnitude under-prediction, we have increased the electron density, n_e, by a factor of three since the SSC intensity is proportional to the square of that quantity. The resulting SEDs are shown in Figure 3 for the instantaneous spectra (solid lines) and the time-averaged spectrum (dashed line). To enable a direct comparison, we also plot the initial instantaneous spectrum from Figure 2 to serve as a proxy for the MAGIC data (dotted curve). Increasing the electron density has brought the time-averaged spectrum closer to this reference curve, but of course there are other differences in detail to consider, particularly with regard to the location of the peak of the SSC spectrum.

Temporal variations in different energy bands can also be used to constrain the model calculations. In Figure 4, we plot our model light curves for the four bands studied by Albert *et al.*, 0.15–0.25 (solid), 0.25–0.6 (dotted), 0.6–1.2 (dashed), and 1.2–10 (dot-dashed) TeV, normalized to a peak flux of unity. Since we are injecting the input electron distribution instantaneously, these light curves all rise simultaneously with zero rise-time. As we note above, the higher energy electrons will have the fastest cooling time scales, and this is seen in the energy-dependence of the light curve decay time scales: the highest energy band decays by about a factor of 2 faster than the lowest band.

Overall, the decay time scales are probably somewhat longer than those seen in the MAGIC data. However, the peak of our time-averaged SSC SED is also low by a factor of $\sim$ 10, indicating that the high energy cut-off of the underlying electron distribution is too low by a factor of 3 or so. In Albert et al., the electron distribution was modeled to have a strong break at $\gamma_b = 10^6$, presumably in order to fit the spectral curvature in the MAGIC spectra [3]. If we increase the break energy of the electrons, this will enable our time-averaged spectrum to fit the MAGIC data better, and it will also increase the SSC loss rates on average for the highest energy electrons and will thereby decrease the decay times. We are currently probing parameter space and including time-dependent injection to determine which model parameters best fit the MAGIC flare data for Mrk 501 in the context of a fully time-evolved calculation [4].
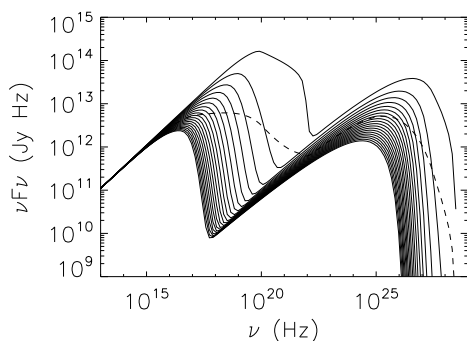
Figure 2: Instantaneous (solid) and time-averaged (dashed) SEDs obtained from our model calculations using the input parameters from Albert *et al.*(2007) [3] for Mrk 501 data during the June 30, 2005 flare.
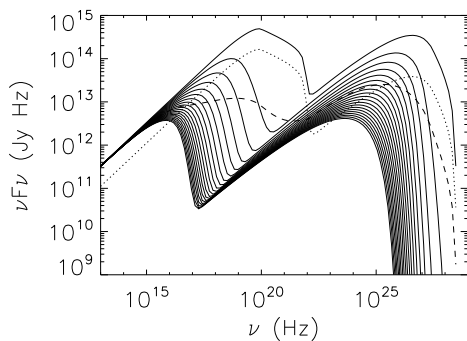
Figure 3: Same parameters as Figure 2, except that we have increased the electron density by a factor of 3. We also show the initial instantaneous SED from Figure 2 to serve as a proxy for the MAGIC data for this flare (dotted).
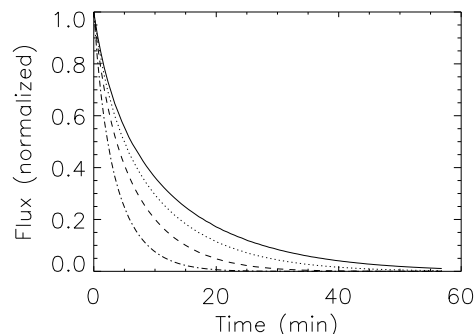
Figure 4: Light curves from our Synch-SSC calculation for the Mrk 501 with the electron density increased by a factor 3. All the curves have been normalized to unity so that the differing decay time scales can be clearly seen. We plot the model light curves for the same bands considered by Albert *et al.* (2007) [3]: 0.15–0.25 (solid), 0.25–0.6 (dotted), 0.6–1.2 (dashed), and 1.2–10 (dot-dashed) TeV. See the text for details.

External Compton Modeling

The previous section presented results based on a pure synchrotron/SSC model, with no external sources of seed photons. Such a model is appropriate to high-energy-peaked BL Lac objects (HBLs), the brightest blazars at TeV energies. However, flat spectrum radio quasars, which are expected to be the brightest sources for GLAST LAT, are likely to have a significant inverse-Compton flux contribution due to seed photons from the accretion disk (ECD and ECC, *cf.* Hartman *et al.* (2001) [5]). The full model includes the contributions from two external sources of seed photons: direct disk emission and disk photons that scatter off the BLR; see Carson & Chiang (2007) [6] for a complete derivation of these two contributions. In this section, we focus specifically on two ways to probe and constrain the physics of the BLR with the model plus high-energy observations.

Probing BLR geometry

Past modeling of the ECC emission has considered only a fairly simple geometry for the BLR material: Thomson or resonant line scattering gas that is
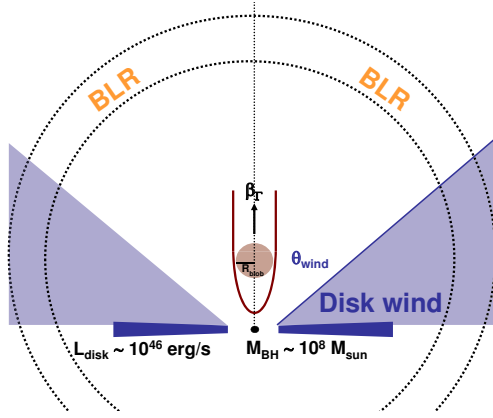
Figure 5: Cartoon of the large-scale view of the AGN, in which the jet is ejected up away from the black hole; both the spherically-distributed cloud geometry and the disk wind geometry are depicted.

spherically distributed about the central black hole. However, optical and UV observations of Seyfert galaxies and radio-quiet quasars, as well as theoretical models, suggest that the BLR material may have a very different geometry, such as an equatorial disk wind [7]. To test this hypothesis, we have modeled the disk wind by introducing an angular dependence (θ_{wind}) into the ECC calculations and evacuating a conical area around the jet (see Figure 5). The geometry of the remaining region, with $\theta_{\mathrm{wind}} \lesssim 30°$, is similar to a wind geometry. We also set the inner radius to $100R_g$ (7×10^{-6} pc for a black hole mass of $1.5 \times 10^8 M_\odot$), adopt $\theta_{\mathrm{wind}} = 0.5$, and introduce a density gradient $n \propto r^{-2}$. We are currently working to assess the observational differences in the SEDs for the two geometries.

BLR effects on the SSC spectrum

The observed ECC flux depends more strongly on the Doppler factor D than the observed SSC emission: $F_{\nu,ECC} \propto D^{4+2\nu}$ and $F_{\nu,SSC} \propto D^{3+\nu}$, where ν is the energy spectral index [8]. Between observing angles of $2°$ and $15°$ the observed ECC flux will decrease by about an order of magnitude relative to the SSC flux. Therefore, even at moderate viewing angles, the SSC emission likely will dominate the *observed* high-energy emission even when there is a lot of BLR material. In cases

where the blazar is pointed sufficiently off-axis so that there is no ECC component to the high-energy peak of the SED, the presence of BLR cooling will change the shape of the high-energy SED hump via its effect on the SSC cooling. We are currently investigating the effects of ECC cooling on the observed SSC spectrum.

Conclusions

We have presented some preliminary results from our leptonic model for the inverse-Compton emission from the inner jets of blazars. As can be seen from our modeling of the June 30, 2007 flare of Mrk 501, the time-averaged SED produced by a full evolution code will be quite different from the SED that one obtains when assuming instantaneous emission. We found model parameters (e.g., n_e, γ_b) that could differ by a factor 3 from the values that were obtained from fitting an instantaneous SED. We are working to apply our time evolution blazar code to model those data more precisely. We are also including more complicated BLR geometries so that we may use the forthcoming simultaneous observations of FSRQs by the GLAST/LAT and the latest TeV telescopes to constrain models of the BLR with gamma-ray data.

References

[1] Böttcher, M., Mause, H., & Schlickeiser, R. A&A, 324, 395–409 (1997)

[2] Böttcher, M. and Bloom, S. D. ApJ, 119, 469–477 (2000)

[3] Albert, J. *et al.*astro-ph/07020008v2 (2007)

[4] Chiang, J., *et al.* 2007, in preparation

[5] Hartman, R. C. *et al.*, ApJ, 553, 683–694 (2001)

[6] Carson, J. E. & Chiang, J. 2007, in preparation

[7] Murray, N., Chiang, J., Grossman, S. A., & Voit, G. M., ApJ, 451, 498 (1995)

[8] Dermer, C. D. ApJ, 446, L63–L66 (1995)